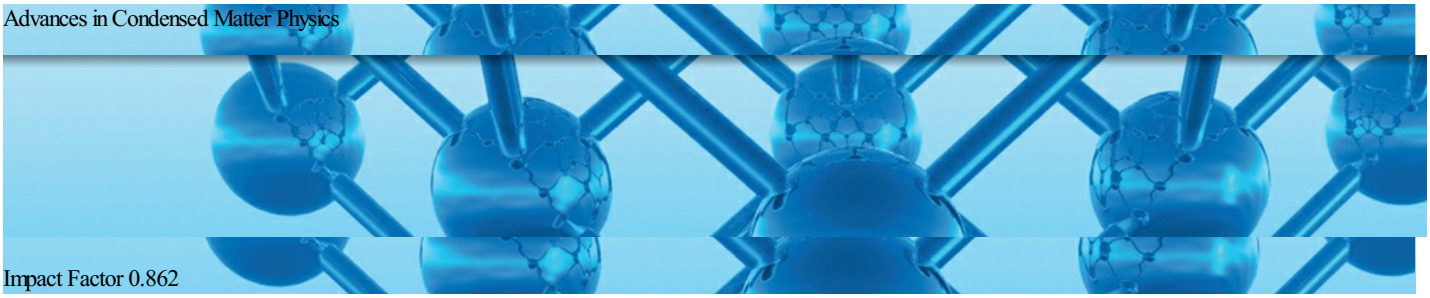

Advances in Condensed Matter Physics
Volume 2013 (2013), Article ID 415726, 6 pages
http://dx.doi.org/10.1155/2013/415726

Research Article

Electronic Structure and Momentum Density of BaO and BaS

R. Kumar,[1] B. K. Sharma,[1,2] and G. Sharma[3]

[1]Department of Physics, University of Rajasthan, Jaipur 302004, India
[2]Faculty of Sciences, Manipal University Jaipur, Jaipur 302007, India
[3]Department of Pure & Applied Physics, University of Kota, Kota 324010, India

Received 25 May 2013; Accepted 24 August 2013

Academic Editor: Dilip Kanhere

Abstract

The electronic structure and electron momentum density distribution in BaO and BaS are presented using Compton spectroscopy. The first-ever Compton profile measurements on polycrystalline BaO and BaS were performed using 59.54 keV gamma-rays. To interpret the experimental data, we have computed the theoretical Compton profiles of BaO and BaS using the linear combination of atomic orbitals method. In the present computation, the correlation scheme proposed by Perdew-Burke-Ernzerhof and the exchange scheme of Becke were considered. The hybrid B3PW and Hartree-Fock based profiles were also computed for both compounds. The ionic configurations are performed to estimate the charge transfer on compound formation, and the present study suggests charge transfer from Ba to O and S atoms. On the basis of equal-valence-electron-density profiles, it is found that BaO is more ionic as compared to BaS.

1. Introduction

The II–VI alkaline earth compounds have interesting bond characteristics and simple crystal structures. BaO and BaS have potential applications in light-emitting diodes (LEDs), laser diodes (LDs), and magnetooptical devices [1–4]. BaO is an indirect bandgap, whereas BaS is a direct bandgap material. At normal conditions, BaO and BaS crystallize in NaCl (B1) structure, but under pressure, they show structural phase transition from B1 to B2 structure [5, 6]. Using the full-potential linearized augmented plane wave (FP-LAPW) method, Drablia et al. [7] reported the electronic and optical properties of BaO and BaS in cubic phase at normal and under hydrostatic pressure. Lin et al. [8] observed that the electronic structure of these compounds containing oxygen atoms always obeys a different relationship from the compounds not containing oxygen atoms using density functional theory (DFT).

Most of the earlier studies, both experimental and theoretical, involve the electronic, optical, and structural properties of BaO and BaS [5–15]. To the best of our knowledge, no one attempted the electronic structure and momentum density of BaO and BaS using Compton spectroscopy. It is well established that Compton spectroscopy provides a useful test to examine the bonding in solids [16, 17]. Thus, we found it worth to study the electronic structure in BaO and BaS using Compton profile. The Compton profile, $J(p_z)$, is related to the ground state electron momentum density $n(\mathbf{p})$ as [16, 17]

$$J(p_z) = \iint_{-\infty}^{+\infty} n(\mathbf{p})\, dp_x dp_y, \quad (1)$$

where integration is performed over a constant-p_z plane, z is scattering vector direction, and $n(\mathbf{p})$ is given as

$$n(\mathbf{p}) \alpha \sum_i \left| \int \psi_i(\mathbf{r}) \exp(-i\mathbf{p}\cdot\mathbf{r})\, d\mathbf{r} \right|^2, \quad (2)$$

where $\psi_i(\mathbf{r})$ is the electron wave function and summation extends over all occupied states. In this paper, the results of a Compton scattering study on BaO and BaS are presented. For the theoretical Compton profiles, first-principles calculations based on linear combination of atomic orbitals (LCAO) method are performed using CRYSTAL06 code [18]. The ionic model has been applied to estimate the charge transfer in these compounds. The nature of bonding in isostructural and isovalent BaO and BaS is also compared using equal-valence-electron-density (EVED) profiles. The paper is organized as follows. Section 2 gives the experimental details and data analysis. The theoretical calculations are presented in Section 3 and Section 4 is devoted to the results and discussion. Finally, the conclusions are drawn in Section 5.

2. Experimental Details and Data Analysis

The measurements on BaO and BaS were performed using 5 Ci ^{241}Am gamma-rays Compton spectrometer. The details of the experimental setup are available in [19]. The incident gamma-rays of 59.54 keV were scattered at an angle of 166° ± 3.0° by the polycrystalline sample of BaO and BaS (pellet of 18 mm dia, 3.2 mm thickness, and effective density for BaO 2.9329 gm/cm^3 and BaS 1.7815 gm/cm^3). The scattered radiation was analyzed using an HPGe detector (Canberra model, GL0110S) which was cooled with liquid nitrogen providing overall momentum resolution of 0.6 a.u. The spectra were recorded with a multichannel analyzer (MCA) with 4096 channels. The calibration of the spectrometer was checked regularly using weak ^{241}Am gamma-rays source. The Compton spectra were measured for BaO near about 48.529 h to collect 2×10^4 counts and BaS around 56.25 h to collect 2.5×10^4 counts at the Compton peak. To deduce the true Compton profile, the raw data were processed for several systematic corrections like background, instrumental resolution, sample absorption, scattering cross-section, and multiple scattering using the computer code of the Warwick Group [20, 21]. Finally, the corrected profiles were normalized to 23.200 for BaO and 26.434 for BaS electrons in the range of 0 to +5 a.u., being the area of free atom Compton profile [22] in the given range. The 1 s electrons of Ba were neglected for both compounds since these do not contribute in the present experimental setup.

3. Theoretical Details

3.1. DFT-LCAO Method

To compute the theoretical Compton profiles of BaO and BaS, the LCAO method embodied in the CRYSTAL06 code [18, 23] was employed. This code provides a platform to calculate electronic structure of periodic systems considering Gaussian basis sets. In the LCAO technique, each crystalline orbital is built from the linear combination of Bloch functions. The Bloch functions are defined in terms of local functions constructed from the atom-centered certain number of Gaussian functions. For Ba, O, and S, the local functions were constructed from the Gaussian type basis sets [24]. In the present DFT calculation, the crystal Hamiltonian was generated using the correlation functional proposed by Perdew et al. [25] and exchange scheme of Becke [26]. The hybrid B3PW and Hartree-Fock (HF) based profiles were also computed for both compounds [18]. The computations were performed by taking B1 structure and 145 k points in the irreducible wedge of the Brillouin zone for BaO and BaS.

3.2. Ionic Model

The theoretical ionic profiles of BaO and BaS for various charge transfer configurations were calculated from the free atom Compton profiles of Ba, O, and S atoms [22]. The valence profiles for various $(Ba)^{+x}(O^{-x})$ and $(Ba)^{+x}(S^{-x})(0.0 \le x \le 2.0)$ configurations were computed by transferring x electrons from the s shell of Ba to the p shell of O and S atoms. The valence profiles for $(Ba)^{+x}(O^{-x})$ and $(Ba)^{+x}(S^{-x})$ configurations were then added to the core contribution to get total profiles. All

these profiles were then convoluted and normalized to compare with the measured profiles of BaO and BaS.

4. Results and Discussion

The numerical values of unconvoluted spherically averaged theoretical Compton profiles (DFT-PBE, B3PW, HF, and Ionic) of BaO and BaS are presented in Table 1. The experimental Compton profiles of BaO and BaS are also given in the table including experimental errors at selected points.

Table 1: The unconvoluted theoretical (DFT-PBE, DFT-B3PW, HF, and Ionic) and experimental Compton profiles for BaO and BaS. The experimental errors at few points are also presented, and all profiles are normalized to the free atom area.

In Figures 1 and 2, the experimental Compton profiles of BaO and BaS are compared with various ionic arrangements to estimate the charge transfer. For a quantitative comparison of the ionic and experiment, the difference profiles $\Delta J = J^{\text{Theory}}(p_z) - J^{\text{Expt}}(p_z)$ have been deduced after convoluting all ionic profiles with a Gaussian function of 0.6 a.u. FWHM. All ionic profiles are normalized to 23.200 electrons for BaO and 26.434 electrons for BaS in the range of 0 to +5 a.u. Figure 1 depicts that the effect of charge transfer from Ba to O atoms is largely visible within 0.0 to 3.0 a.u. for BaO. The best agreement is found for $x = 1.0$. Figure 2 shows that the charge transfer configuration $x = 1.5$ is closet to the experiment for BaS. Beyond 3.0 a.u., all configurations show identical behavior for both compounds. On the basis of χ^2 checks and from Figures 1 and 2, it is found that $Ba^{+1.0}O^{-1.0}$ and $Ba^{+1.5}S^{-1.5}$ configurations give the best agreement for BaO and BaS, respectively. Thus, the model suggests the transfer of 1.0 and 1.5 electrons from the valence s state of Ba to the p states of O and S for BaO and BaS, respectively.

Figure 1: Difference (ΔJ) between convoluted ionic and experimental Compton profiles of BaO. Experimental errors ($\pm\sigma$) are also shown at points. All ionic profiles are convoluted with the Gaussian of 0.6 a.u. FWHM.

Figure 2: Difference (ΔJ) between convoluted ionic and experimental Compton profiles of BaS. Experimental errors ($\pm\sigma$) are also shown at points. All ionic profiles are convoluted with the Gaussian of 0.6 a.u. FWHM.

The differences $(\Delta J = J^{\text{Theory}}(p_z) - J^{\text{Expt}}(p_z))$ between experimental and LCAO scheme based Compton profiles are presented in Figures 3 and 4 for BaO and BaS, respectively. Figure 3 shows that for BaO all theories (DFT-PBE, B3PW, and HF) predict lower momentum density as compared to experiment in the momentum range of $0.0 < p_z < 0.5$ a.u., while the trend reversed in the momentum range of $0.5 < p_z < 2.0$ a.u. The difference between theory and experiment is negligible in the high momentum region, because the contribution in this region is mostly due to core electrons, which remain unaffected in the compound formation. Similar features are also visible in Figure 4, but the effect of exchange and correlation is not seen for BaS.

Figure 3: The difference of DFT-PBE, B3PW, and HF with experimental Compton profile of BaO. All profiles are convoluted with the Gaussian of 0.6 a.u. FWHM.

Figure 4: The difference of DFT-PBE, B3PW, and HF with experimental Compton profile of BaS. All profiles are convoluted with the Gaussian of 0.6 a.u. FWHM.

The directional Compton profiles of BaO and BaS along [100], [110], and [111] directions have been computed to examine the anisotropies [100]–[110], [110]-[111], and [100]–[111] in the electron momentum density. All these anisotropies are derived from convoluted B3PW hybrid scheme and presented in Figures 5 and 6 for BaO and BaS, respectively. Figure 5 depicts that all anisotropies are positive in nature at $p_z = 0.0$ a.u. for BaO. It indicates larger occupied states along [100] direction with low momentum. A close inspection of this figure reveals that maximum anisotropy is seen between [100] and [111] directions at 0.6 a.u. and 1.2 a.u. All anisotropies are visible up to 3.0 a.u. In Figure 6, the anisotropies are plotted for BaS. This figure shows similarity with BaO, but all anisotropies are diminished beyond 2.0 a.u. Measurements on single crystalline samples of BaO and BaS along principal directions would be valuable to examine these findings.

Figure 5: Directional anisotropies, $\Delta J(p_z)$, for BaO for the pair of directions [100]–[110], [110]-[111], and [100]–[111].

Figure 6: Directional anisotropies, $\Delta J(p_z)$, for BaS for the pair of directions [100]–[110], [110]-[111], and [100]–[111].

The nature of bonding in isostructural and isovalent BaO and BaS has been compared and plotted in Figure 7. In this figure, the experimental EVED profiles of these compounds are considered. We also plot the theoretical EVED profiles in the inset. The EVED profiles were derived by normalizing valence electron profiles to 4.0 electrons and scaling the resulting profiles by the Fermi momentum (p_F). For BaO and BaS, p_F turned out to be 0.938 and 0.813 a.u., respectively, using the expression $(3\pi^2 n)^{1/3}$, where n is the valence electron density. A number of researchers have proved that this scheme offers a way to understand the nature of bonding in isovalent and isostructural compounds [27–31]. It is seen from Figure 7 that, near $p_z = 0$ a.u., the sharpness of Compton profiles is higher for BaS, which suggests more localization of charges in BaS in the bonding direction as compared to BaO. It is worth mentioning here that the covalent bonding is a result of sharing of electrons, and hence, it increases localization of charge in bonding direction which results in a sharper Compton line shape [32, 33]. Therefore, we conclude that the ionic character is higher for BaO as compared to BaS. The larger ionic character of BaO as compared to BaS is well supported by the bulk modulus and cohesive energy data [34].

Figure 7: The equal-valence-electron-density (EVED) profiles of BaO and BaS ($p_F = 0.938$ and 0.813 a.u., resp.). These profiles are deduced from the experimental valence profiles. The inset shows the EVED profiles derived from the theoretical valence profiles of these compounds. All these profiles are normalized to 4.0 electrons.

5. Conclusions

Electronic structure and momentum density in BaO and BaS using Compton scattering technique are reported. The experimental values of Compton profiles are compared with the LCAO based values for both compounds. The anisotropies in momentum densities depict larger occupied states along [100] direction with low momentum. In addition, the ionic model based calculations have also been used to estimate the charge transfer in the compounds, and the model suggests a transfer of 1.0 and 1.5 electrons from s state of Ba atom to p state of O and S atoms. The EVED profiles for the compounds conclude higher ionic character in BaO as compared to BaS.

Acknowledgments

This work is financially supported by the CSIR, New Delhi, through the Grant no. 03(1205/12EMR-II). G. Sharma is also thankful to the Head of the Department of Pure & Applied Physics, University of Kota, Kota, for providing the computational facilities.

References

1. P. Cervantes, Q. Williams, M. Côté, M. Rohlfing, M. L. Cohen, and S. G. Louie, "Band structures of CsCl-structured BaS and CaSe at high pressure: implications for metallization pressures of the alkaline earth chalcogenides," *Physical Review B*, vol. 58, no. 15, pp. 9793–9800, 1998. View at Google Scholar · View at Scopus
2. T. Lv, D. Chen, and M. Huang, "Quasiparticle band structures of BaO and BaS," *Journal of Applied Physics*, vol. 100, Article ID 086103, 3 pages, 2006. View at Publisher · View at Google Scholar
3. S. Drablia, H. Meradji, S. Ghemid, G. Nouet, and F. El Haj Hassan, "First principles investigation of barium chalcogenide ternary alloys," *Computational Materials Science*, vol. 46, no. 2, pp. 376–382, 2009. View at Publisher · View at Google Scholar · View at Scopus
4. M. Uludoan, T. Çain, A. Strachan, and W. A. Goddard III, "Ab-initio studies of pressure induced phase transitions in BaO," *Journal of Computer-Aided Materials Design*, vol. 8, no. 2-3, pp. 193–202, 2001. View at Publisher · View at Google Scholar · View at Scopus
5. M. Alfredsson, J. P. Brodholt, P. B. Wilson et al., "Structural and magnetic phase transitions in simple oxides using hybrid functionals," *Molecular Simulation*, vol. 31, no. 5, pp. 367–377, 2005. View at Publisher · View at Google Scholar · View at Scopus
6. S. T. Weir, Y. K. Vohra, and A. L. Ruoff, "High-pressure phase transitions and the equations of state of BaS and BaO," *Physical Review B*, vol. 33, no. 6, pp. 4221–4226, 1986. View at Publisher · View at Google Scholar · View at Scopus
7. S. Drablia, H. Meradji, S. Ghemid, N. Boukhris, B. Bouhafs, and G. Nouet, "Electronic and optical properties of BaO, BaS, BaSe, BaTe and BaPo compounds under hydrostatic pressure," *Modern Physics Letters B*, vol. 23, no. 26, pp. 3065–3079, 2009. View at Publisher · View at Google Scholar · View at Scopus
8. G. Q. Lin, H. Gong, and P. Wu, "Electronic properties of barium chalcogenides from first-principles calculations: tailoring wide-band-gap II-VI semiconductors," *Physical Review B*, vol. 71, no. 8, Article ID 085203, 2005. View at Publisher · View at Google Scholar · View at Scopus
9. M. Ameri, A. Touia, H. Khachai, Z. Mahdjoub, M. Z. Chekroun, and A. Slamani, "Ab initio study of structural and electronic properties of barium chalcogenide alloys," *Materials Sciences and Applications*, vol. 3, pp. 612–618, 2012. View at Google Scholar
10. Y. Kang, Y. S. Kim, Y. C. Chung, H. Kim, D. S. Kim, and J. J. Kim, "The evaluation of ultrasoft pseudopotential in predicting material properties of ionic systems by an ab-initio pseudopotential method," *Journal of Ceramic Processing Research*, vol. 3, no. 3, pp. 171–173, 2002. View at Google Scholar · View at Scopus
11. R. K. Singh, A. S. Verma, and S. K. Rathi, "Ground state properties of rock salt, CsCl, diamond and zinc blende structured solids," *The Open Condensed Matter Physics Journal*, vol. 2, pp. 25–29, 2009. View at Publisher · View at Google Scholar
12. M. Teng and X. Hong, "Phase transition and thermodynamic properties of BaS: an Ab initio study," *Wuhan University Journal of Natural Sciences*, vol. 16, no. 1, pp. 33–37, 2011. View at Publisher · View at Google Scholar · View at Scopus
13. F. El Haj Hassan and H. Akbarzadeh, "First-principles elastic and bonding properties of barium chalcogenides," *Computational Materials Science*, vol. 38, no. 2, pp. 362–368, 2006. View at Publisher · View at Google Scholar · View at Scopus
14. R. Khenata, M. Sahnoun, H. Baltache et al., "Structural, electronic, elastic and high-pressure properties of some alkaline-earth chalcogenides: an ab initio study," *Physica B*, vol. 371, no. 1, pp. 12–19, 2006. View at Publisher · View at Google Scholar · View at Scopus
15. Z. Feng, H. Hu, Z. Lv, and S. Cui, "First-principles study of electronic and optical properties of BaS, BaSe and BaTe," *Central European Journal of Physics*, vol. 8, no. 5, pp. 782–788, 2010. View at Publisher · View at Google Scholar · View at Scopus
16. M. J. Cooper, P. E. Mijnarends, N. Shiotani, N. Sakai, and A. Bansil, *X-Ray Compton Scattering*, Oxford Publishing Press, Oxford, UK, 2004.
17. M. J. Cooper, "Compton scattering and electron momentum determination," *Reports on Progress in Physics*, vol. 48, no. 4, pp. 415–481, 1985. View at Publisher · View at Google Scholar
18. R. R. Dovesi, V. R. Saunders, C. Roetti et al., *CRYSTAL06 User's Manual*, University of Torino, Torino, Canada, 2006.
19. B. K. Sharma, A. Gupta, H. Singh, S. Perkkiö, A. Kshirsagar, and D. G. Kanhere, "Compton profile of palladium," *Physical Review B*, vol. 37, no. 12, pp. 6821–6826, 1988. View at Publisher · View at Google Scholar · View at Scopus
20. D. N. Timms, *Compton scattering studies of spin and momentum densities [Ph.D. thesis]*, University of Warwick, Coventry, UK, 1989.
21. J. Felsteiner, P. Pattison, and M. Cooper, "Effect of multiple scattering on experimental Compton profiles: a Monte Carlo calculation," *Philosophical Magazine*, vol. 30, no. 3, pp. 537–548, 1974. View at Google Scholar · View at Scopus
22. F. Biggs, L. B. Mendelsohn, and J. B. Mann, "Hartree Fock Compton profiles for the elements," *Atomic Data and Nuclear Data Tables*, vol. 16, no. 3, pp. 201–309, 1975. View at Google Scholar · View at Scopus
23. R. Dovesi, R. Orlando, C. Roetti, C. Pisani, and V. R. Saunders, "The periodic Hartree-Fock method and its implementation in the CRYSTAL code," *Physica Status Solidi B*, vol. 217, no. 1, pp. 63–88, 2000. View at Google Scholar · View at Scopus
24. http://www.tcm.phy.cam.ac.uk/.
25. J. P. Perdew, K. Burke, and M. Ernzerhof, "Generalized gradient approximation made simple," *Physical Review Letters*, vol. 77, no. 18, pp. 3865–3868, 1996. View at Google Scholar · View at Scopus
26. A. D. Becke, "Density-functional exchange-energy approximation with correct asymptotic behavior," *Physical Review A*, vol. 38, no. 6, pp. 3098–3100, 1988. View at Publisher · View at Google Scholar · View at Scopus
27. M. C. Mishra, G. Sharma, R. K. Kothari, Y. K. Vijay, and B. K. Sharma, "Electronic structure of CaX (X = O, S, Se) compounds using Compton spectroscopy," *Computational Materials Science*, vol. 51, no. 1, pp. 340–346, 2012. View at Publisher · View at Google Scholar · View at Scopus
28. N. Munjal, G. Sharma, V. Vyas, K. B. Joshi, and B. K. Sharma, "Ab-initio study of structural and electronic properties of AlAs," *Philosophical Magazine*, vol. 92, pp. 3101–3112, 2012. View at Publisher · View at Google Scholar
29. G. Sharma, K. B. Joshi, M. C. Mishra et al., "Electronic structure of AlAs: a Compton profile study," *Journal of Alloys and Compounds*, vol. 485, no. 1-2, pp. 682–686, 2009. View at Publisher · View at Google Scholar · View at Scopus
30. R. Kumar, N. Munjal, G. Sharma, V. Vyas, M. S. Dhaka, and B. K. Sharma, "Electron momentum density and phase transition in SrO," *Phase Transitions*, vol. 85, no. 12, pp. 1098–1108, 2012. View at Publisher · View at Google Scholar
31. W. A. Reed and P. Eisenberger, "Gamma-ray compton profiles of diamond, silicon, and germanium," *Physical Review B*, vol. 6, no. 12, pp. 4596–4604, 1972. View at Publisher · View at Google Scholar · View at Scopus
32. G. Sharma, K. B. Joshi, M. C. Mishra, S. Shrivastava, Y. K. Vijay, and B. K. Sharma, "Electron momentum density in multiwall carbon nanotubes," *Physica E*, vol. 43, no. 5, pp. 1084–1086, 2011. View at Publisher · View at Google Scholar · View at Scopus
33. M. C. Mishra, R. Kumar, G. Sharma, Y. K. Vijay, and B. K. Sharmab, "Size dependent electron momentum density distribution in ZnS," *Physica B*, vol. 406, no. 22, pp. 4307–4311, 2011. View at Publisher · View at Google Scholar · View at Scopus
34. A. S. Verma, "An empirical model for bulk modulus and cohesive energy of rocksalt-, zincblende- and chalcopyrite-structured solids," *Physica Status Solidi B*, vol. 246, no. 2, pp. 345–353, 2009. View at Publisher · View at Google Scholar · View at Scopus